3d-5d band magnetism in rare earth-transition metal intermetallics: total and partial magnetic moments of the RFe$_2$ (R=Gd-Yb) Laves phase compounds

3d–5d band magnetism in rare earth–transition metal intermetallics: total and partial magnetic moments of the RFe$_2$ (R = Gd–Yb) Laves phase compounds

M S S Brooks[†‡], Lars Nordström[‡] and Börje Johansson[‡]

† Commission of the European Communities, European Institute for Transuranium Elements, Postfach 2340, D-7500 Karslruhe, Federal Republic of Germany
‡ Condensed Matter Theory Group, Department of Physics, University of Uppsala, Box 530, S-751 21 Uppsala, Sweden

Abstract. The magnetic moments of the RFe$_2$ (R = Gd–Yb) Laves phase compounds have been calculated. Agreement with published measured values for single crystals is excellent. The R 4f magnetic moments were obtained from the standard Russell–Saunders scheme but the radial 4f spin density was otherwise part of the self-consistent density functional calculation. The influence of the localized 4f magnetism upon the conduction band magnetism is examined in detail and exchange interactions extracted. The site- and angular-momentum-resolved contributions to the total conduction bands magnetic moments are calculated and shown to obey an approximate sum rule which conserves the total conduction band moment, despite the change of 4f moment, across the series.

1. Introduction

In a previous paper (Brooks *et al* 1989—to be referred to as I) we examined in detail 3d–5d hybridization, spin transfer to 5d bands and site-resolved and total magnetic moments in LuFe$_2$. In addition, we proposed a model of the magnetism in rare earth compounds for which the rare earth (R) has a 4f moment. In this model, which is close to that proposed by Campbell (1972) on heuristic grounds, the R 4f spin density polarizes the R 5d states through local exchange interactions but is otherwise isolated from the conduction electron environment. Campbell postulated local 4f–5d exchange interactions and direct d–d interactions of an undefined nature but similar to d–d interactions in transition metals. We find that the intersite interactions are entirely due to 5d–3d hybridization. We also suggested in I that, if the 4f spin density could be calculated accurately, then the local spin density approximation (LSDA) to density functional theory (Hohenburg and Kohn 1964, Kohn and Sham 1965) could be used—in the form of self-consistent energy band calculations for all valence electron states except the 4f states—to compute the spin densities in any rare earth compounds for which the local 4f spin moment was known. The purpose of the present paper is to report such calculations for the RFe$_2$ (R = Gd–Yb) series.

The main problem in a density functional treatment of the combination of localized 4f magnetism and the itinerant, predominantly 3d–5d, magnetism in rare earth–transition

metal (M) intermetallics is to know how to handle the 4f spin density in LSDA. This problem for the case of the elemental metals has been reviewed by Harmon (1979). Early practice had been to treat the 4f states as part of a paramagnetic core (Dimmock and Freeman 1964, Keaton and Loucks 1966) since, at that time, LSDA was not available—but more recently they have been treated as part of the band structure (Harmon 1979, Sticht and Kübler 1985, Temmerman and Sterne 1990). We are not convinced that the latter practice is either correct or necessary when the 4f moments appear to be well-described by Russell–Saunders coupling and the 4f states well to the localized side of a Mott transition. The former practice suppresses 4f magnetism altogether. It is, however, a simple matter to spin polarize the 4f density and include the 4f spin densities in the total spin density. In this manner the influence of the 4f moments upon the magnetism is calculated *ab initio* although the choice of 4f occupation number and moment is not. It is this method that is used in the present work and its implementation is discussed in detail in section 2.

The self-consistent LMTO energy band technique in the atomic sphere approximation (ASA) used in the present work was described in I. A full description of the LMTO method may be obtained from the publications of Andersen and his collaborators (Andersen 1975, Andersen *et al* 1985, Skriver 1983). When only the spherically symmetric spin densities in each atomic sphere are iterated the choice of atomic sphere sizes can be important. In the present work we have tried to choose the Wigner–Seitz radii in a consistent manner. The Fe Wigner–Seitz radius was chosen to be 1.418 Å throughout the series, as in Fe metal with an FCC structure, and the R radius chosen to yield the correct lattice parameter. The crystal data and Wigner–Seitz radii used in the calculations are compiled in table 1.

In section 3 the main numerical results are discussed and the calculated and measured magnetic moments compared. Agreement with experiment is excellent and we are able to develop an understanding of how the R 4f moment influences the site-resolved conduction electron moments. The most important result is that, although the total conduction electron moment does not change much across the series, the R 5d and M 3d moments—which are anti-parallel—increase linearly with increasing R 4f moment.

In section 4 we examine the influence of the R 4f moments upon the exchange splittings of the 5d and 3d bands and compare the latter with the LSDA exchange integrals. In section 5 a simple model of 3d–5d hybridization is used to explain the conservation of total conduction electron moment across the series and the problem of flipping the 5d spin in a uniform magnetic field is addressed. Finally, in section 6, we summarize what we have learnt from the present work and generalize this to the technically important class of magnetic materials R_xM_y.

2. Spin-polarized 4f states and their influence upon the conduction electron band structure

Although LSDA is used primarily in the study of magnetism in solids, it has also been used successfully to calculate the total energies of free atoms (Gunnarsson *et al* 1974, Moruzzi *et al* 1978). The energy associated with Hund's first rule appears in LSDA as the spin-polarization energy, E_{sp}, which is the energy difference between the atom with no net spin and the atom with the maximum possible net spin (subject to the Pauli principle) in the open shells (Johansson *et al* 1980, Brooks and Johansson 1983). Here we shall be interested not so much in the total energy associated with Hund's first rule as with the change in potential due to spin polarization. The exchange and correlation energy,

E_{xc}, is in general a function of the spin-up and spin-down densities, $n^+(r)$ and $n^-(r)$, respectively. In LSDA the exchange and correlation potential is—here we use the parametrization of von Barth and Hedin (1972)—given by

$$v_{xc}^{\pm}(r) = A(n(r))(2n^{\pm}(r)/n(r))^{1/3} + B(n(r)) \tag{2.1}$$

where A and B are functionals of the total electron density, $n(r) = n^+(r) + n^-(r)$ (von Barth and Hedin 1972). Since the total spin-up and spin-down potentials contain $v_{xc}^{\pm}(r)$ additively, the difference between spin-up and spin-down potentials is

$$\Delta v_{xc} = v_{xc}^+(r) - v_{xc}^-(r). \tag{2.2}$$

Here we see the origin of exchange interactions in LSDA. The difference between the spin-up and spin-down potentials is a functional of the local *total* spin-up and spin-down densities.

In order to describe the combination of localized 4f magnetism and itinerant magnetism of the spd band structure in heavy rare earth–transition metal intermetallics, we treat the localized 4f states as outer core states in the sense that they are not allowed to hybridize with the conduction electron band structure. Thus there is no 4f contribution to the conduction electron state densities. This is done in order that the number of 4f electrons may be fixed to an integer, as in the infinite-U limit of Hubbard's model (Hubbard 1963). Since we shall also fix the total 4f spin, the individual 4f spin-up and spin-down occupation numbers are fixed. Subject to this constraint, the 4f spin densities are calculated self-consistently. The 4f wave spin-up and spin-down wave functions are calculated in the total spin-up and spin-down potentials subject to the condition that their logarithmic derivatives, D_f, at the rare earth Wigner–Seitz sphere boundaries equal $(-l-1)$, which is the appropriate boundary condition for a resonance in ASA. The 4f spin densities contribute to the total spin densities, and hence to the spin-up and spin-down potentials. Clearly, since no 4f–conduction band hybridization is present, the interaction between 4f and conduction electron densities is electrostatic plus local exchange and the entire 4f–conduction band magnetic interaction is local exchange. Since the 4f spin density is highly non-uniform, so is its effect upon the spin-up and spin-down potentials. The effect of exchange with 4f electrons, felt by the conduction electrons, is therefore also highly non-uniform and no approximation of the nature of a Stoner splitting or uniform molecular field need be made in the self-consistent calculations—although we shall show in section 4 that this is a reasonable approximation.

The problem of how to fix the number of spin-up and spin-down 4f electrons remains. The total number of 4f electrons is not a problem as it is known to change from seven for Gd to thirteen for Yb in trivalent compounds. The spin occupation numbers are determined by applying the standard Russell–Saunders' coupling scheme to the 4f shell. Then S is maximized, L is maximized for a given maximum S, and the total momentum J is $J = L + S$. The magnetic moment is given by $\mu_f = g_J J$ where g_J is the Landé factor,

$$g_J = 1 + [J(J+1) + S(S+1) - L(L+1)]/2J(J+1). \tag{2.3}$$

The ground state spin component of the total 4f moment, μ_f^s, is obtained from the projection of the spin along the direction of total angular momentum:

$$\mu_f^s = 2(g_J - 1)J. \tag{2.4}$$

The 4f spin-up and spin-down occupation numbers are then determined by

$$n_f^+ + n_f^- = n_f \qquad n_f^+ - n_f^- = \mu_f^s \tag{2.5}$$

where n_f is the total number of 4f electrons. The results of applying the standard scheme,

which determines $n_{\uparrow}^{+}$, $n_{\uparrow}^{-}$ uniquely, for heavy rare earth metals are summarized in table 1. Clearly the occupation numbers $n_{\uparrow}^{+}$, $n_{\uparrow}^{-}$ are part of the input to the calculations and are not determined *ab initio* as are the partial occupation numbers of the conduction electron states.

The fact that the 4f occupation numbers are not determined *ab initio* will obviously cause difficulty if the Russell–Saunders scheme is not correct. We have, for example, made the non-trivial *ansatz* that the 4f spin density is determined by the projection of the spin along *J* or the total moment direction. For the heavy rare earths, with *L* and *S* parallel, there is no obvious difficulty since the resulting projection of *S* along *J* is equal to *S*. But for the light rare earths, with *S* and *L* anti-parallel, this is not so and the occupation numbers for spin-up and spin-down states must be made non-integral, although their sum is of course integral. Nevertheless, since LSDA in its present form is a mean-field theory, what are required are the spin-up and spin-down potentials along the moment direction and these should be obtained from the quantum mechanical average of the spin density along this direction. Therefore, as long as the Russell–Saunders scheme is reliable, the projection of the spin density along the total moment direction should be the appropriate quantity with which to split the potential. The foregoing is, of course, completely consistent with the de Gennes factor (de Gennes 1962) and model theories of s–f interactions (see, e.g., Liu 1978) where, at the mean-field level, the projection of the 4f spin along the total 4f moment direction enters the 4f–conduction electron exchange interaction.

The Russell–Saunders value for the spin and spin moment may also be incorrect if the crystal field is strong enough to quench the total moment appreciably, or if intermediate coupling is a more appropriate scheme. The latter may be the case in samarium and its compounds where the excited $J = \frac{7}{2}$ state is close to the $J = \frac{5}{2}$ ground state (Buschow *et al* 1973, de Wijn *et al* 1976), whereas the former is more likely to occur when the 4f moment and corresponding exchange splitting is small. What is then required, to be able to apply the kind of theory proposed here, is a detailed knowledge of the 4f ground state in the compound in question. From such a knowledge, the average of the 4f spin moment and its direction could be deduced and inserted in the theory through (2.5). In the present paper we assume that crystal fields are small and that the 4f spin moments are given by (2.3)–(2.5). We then compare the results for the total moments with those measured for RFe_2 single crystals (Clark 1980). Since agreement between experiment and theory turns out to be good, the use of the Russell–Saunders coupling scheme is justified *a posteriori*.

Finally, a common problem that arises whenever the band structures of rare earths are discussed is that the calculated state densities do not compare favourably with optical experiments (Harmon 1979). In the present work there is not even any partial 4f contribution to the conduction electron state density. Even if there were, however, it would undoubtedly have weight in the incorrect place as the 4f states are localized (Herbst *et al* 1972, Johansson 1974, 1979, Gunnarsson and Schönhammer 1983, 1985). Since our objective is to calculate only the spatial 4f ground state densities in order to determine their effect upon the total and site-resolved moments, their spectral composition in the present context is irrelevant. We are therefore restricted to the calculation of ground state properties.

3. Numerical results and comparison with experiment

The self-consistently calculated partial R 5d and M 3d occupation numbers are plotted in figure 1 as a function of the R component of the compound. The number of 3d

Table 1. Crystal and magnetic data input to the self-consistent LMTO calculations. The first column lists the measured lattice constants according to the review article by Buschow (1977). The second column lists the lattice constants actually used in the calculations. The third and fourth columns list the chosen Wigner–Seitz radii. The R 4f moments, their decomposition into spin and orbital contributions according to Russell–Saunders coupling, and the resulting spin-up and spin-down occupation numbers according to (2.5), are shown in the final columns. Distances are in Å and moments in μ_B.

	a_{expt}	a_{theor}	S_R	S_M	μ_{4f}^s	n_{4f}^+	n_{4f}^-	μ_{4f}^l	μ_{4f}
$GdFe_2$	7.396	7.394	1.853	1.418	7	7	0	0	7
$TbFe_2$	7.347	7.348	1.831	1.418	6	7	1	3	9
$DyFe_2$	7.325	7.326	1.820	1.418	5	7	2	5	10
$HoFe_2$	7.304	7.303	1.810	1.418	4	7	3	6	10
$ErFe_2$	7.283	7.282	1.799	1.418	3	7	4	6	9
$TmFe_2$	7.247	7.246	1.781	1.418	2	7	5	5	7
$YbFe_2$	7.239	7.238	1.777	1.418	1	7	6	3	4

electrons/Fe remains more or less constant at about 6.6, but the number of 5d electrons/ R decreases from 1.92 in $GdFe_2$ to 1.68 in $YbFe_2$. This decrease in 5d occupation number is caused by lanthanide contraction. As may be seen from table 1, the decrease in lattice constant with increasing R atomic number is due to the decrease in the size of the R component of the compound, which arises from contraction of the 4f shell. The corresponding increase in the shielding of the 5d states from the nucleus raises their energy and broadens the 5d energy bands. In the elemental rare earth metals the subsequent reduction in 5d occupation number has been shown to be the origin of the crystal structure sequence across the series (Duthie and Pettifor 1977). The mechanism here is slightly different as the increase in energy of the unhybridized 5d bands reduces the 3d–5d hybridization and resulting charge transfer to the 5d states. But the end effect is the same, as the 5d occupation number is reduced by the amount shown in figure 1. Here, where we are trying to study the systematics of the magnetism the dependence of occupation number upon nuclear charge is an inconvenience. Therefore, in order to separate and understand the influence of R 4f magnetism upon the itinerant magnetism, we have added a further set of spin-polarized calculations to those for the real compounds by reducing the 4f moment in $GdFe_2$ monotonically from 7 to 0, keeping, of course, the total 4f occupation number constant. Thus, for $GdFe_2$, we set $n^+ - n^- = \mu_{4f}^s$ with $\mu_{4f}^s = 0, 1, \ldots, 7$. In this way we have a set of calculations (to be called Gd-4f-red) for an ideal system in which the R 4f moment is varied but other variables such as atomic numbers, nuclear charge, and lattice constant are constant.

The comparison between the results for the ideal system, which simulates the RFe_2 series (R = Gd–Yb) with only the 4f moment allowed to vary, and the real compounds will prove to be extremely enlightening. For example, in figure 1, where the R 5d and M 3d occupation numbers are also plotted for Gd-4f-red, it is clear that there is no change in these quantities—which we therefore now know for certain to be influenced not by the 4f moment, but by the changing nuclear charge.

The differences between the centres of the $5d^{\pm}$ and $3d^{\pm}$ bands are plotted for the series in figure 2. This figure, together with table 2 where the bandwidth parameters and second moments of the R 5d–M 3d hybridization structure constants are listed, contains
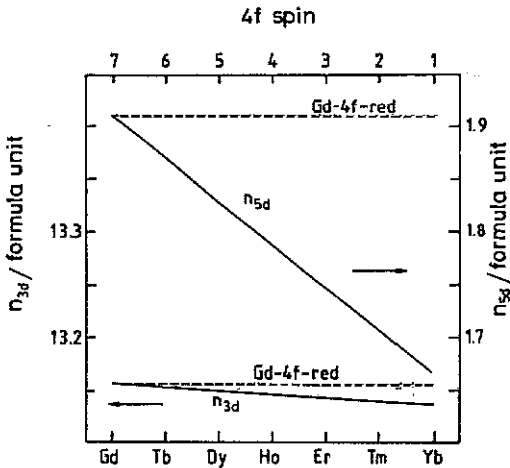
Figure 1. Calculated partial occupation numbers for the R 5d- and M 3d-resolved conduction bands as a function of the rare earth component of the compound. The broken line, labelled Gd-4f-red, is for the ideal system GdFe$_2$ with reduced 4f spin.
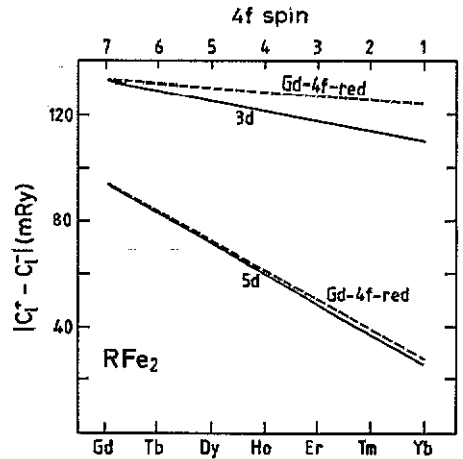

Figure 2. The difference between the spin-up and spin-down band centres (or average Stoner splitting) for the R 5d and M 3d bands. The broken line is again for the ideal system GdFe$_2$ with reduced spin.

Table 2. Calculated potential parametes for the RFe$_2$ series. The Δ_l are the bandwidth parameters and C_l^+, C_l^- the centres of partial spin-up and spin-down bands, respectively. All energies are in mRyd relative to the Fermi level. At the bottom the second moments of the structure constants are given.

	Δ_{5d}	Δ_{3d}	C_{5d}^+	C_{5d}^-	C_{3d}^+	C_{3d}^-
GdFe$_2$	3.5	0.4	209	308	23	−112
TbFe$_2$	3.5	0.4	220	305	20	−111
DyFe$_2$	3.5	0.5	230	302	17	−110
HoFe$_2$	3.4	0.5	239	298	14	−108
ErFe$_2$	3.4	0.5	247	296	10	−106
TmFe$_2$	3.4	0.5	258	296	8	−106
YbFe$_2$	3.4	0.5	267	296	8	−106

$M_{3d-3d}^2 = 1178$, $M_{5d-5d}^2 = 53$, $M_{3d-5d}^2 = 241$

the information essential to the application of the approximate theory of 3d–5d hybridization, charge and moment transfer outlined in I. We shall return to this approximate theory in section 4.

The itinerant magnetism of RFe$_2$ compounds is dominated by R 5d and M 3d magnetism. The calculated 3d and 5d contributions to the total moments are plotted in figure 3. As the R 4f spin component of the moment increases between Yb and Gd, the magnitude of both partial 3d and partial 5d contributions to the total moment increases. However, since the 3d and 5d moments are anti-parallel, the sum of the 3d and 5d moments changes far less. That this is no coincidence, but is in fact due to a sum rule, may be seen from the same plot for Gd-4f-red which is also shown in figure 3. Here the 3d moment changes less across the series and the sum of the 3d and 5d moments remains
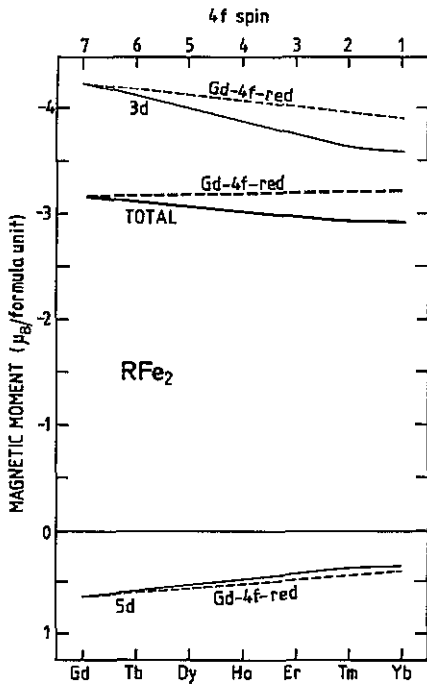
Figure 3. The calculated conduction electron spin contributions to the moments of the RFe$_2$ series. The negative spin for the total and M 3d contribution was chosen because they are anti-parallel to the R 4f moment (table 1) and the total moment is therefore positive.

constant. Therefore, when we isolate the effect of changing only the 4f moment, the total conduction electron moment remains constant due to cancellation of the changes in 3d and 5d moments. We shall discuss this sum rule in more detail in section 4. Here it is sufficient to note that the reason is that the 5d bands are, before hybridization, essentially empty. 5d charge and spin densities are therefore obtained from the 3d bands by hybridization—hence the conservation of total conduction electron charge and moment when only the 4f moment is changed. However, we recall from figure 1 that in the real compounds the 5d occupation number decreases across the series. This additional effect, which is not related to the 4f moment but to lanthanide contraction, makes the sum rule appear incomplete in the real compounds.

By now it should be clear that if only the total moment is measured, and from it the R 4f moment subtracted, the resulting conduction electron moment will be more or less constant across the series, decreasing only slightly from GdFe$_2$ to YbFe$_2$ for the real compounds. If this conduction electron moment were then attributed entirely to the 3d states it would appear as if the 3d moments were more or less constant at about 1.6 μ_B/Fe across the series. This is the conclusion arrived at by Clark (1980) and is the currently accepted view. On the contrary we find that the approximate sum rule for the total 3d–5d moment conceals the change in the site-resolved moments, which may only be obtained from neutron diffraction experiments. Clark's reasoning is quite correct if applied to the sum of the 3d and 5d moments. In table 3 we have summarized the results of our calculations by listing the calculated moments resolved according to atom and orbital character. The only neutron diffraction experiments known to us in which the site resolution of the moments has been made are for HoFe$_2$ (Moreau *et al* 1971, Feuss *et al* 1979)—where an Fe moment of 1.7 μ_B was measured in the first experiment and 1.88(10) μ_B in the latter—and for ErFe$_2$ (Bargouth and Will 1971), where an Fe moment

Table 3. Resolution of the calculated moments for the RFe_2 series into partial contributions resolved by site and angular momentum. The first column contains the R 4f contribution equal to $g_J J$ in Russell–Saunders coupling. The second and third columns are the conduction electron site-resolved contributions. The fourth column contains the total conduction electron moment which, added to column one, yields the total moment. The fifth and sixth columns are the R 5d and M 3d contributions for comparison with neutron diffraction data and the final column contains the diffuse s and p contributions, which are not observable in diffraction experiments. The sums of columns five to seven equal the total conduction electron moments in column four, which are also the sums of columns two and three. All moments are in μ_B/formula unit.

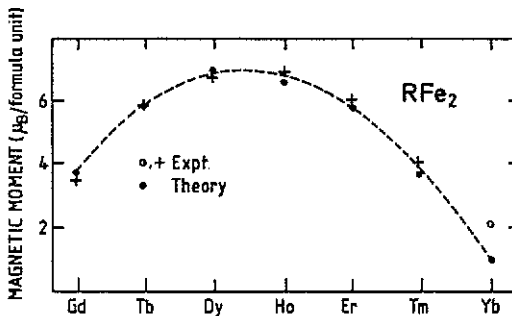|	(1)	(2)	(3)	(4)	(5)	(6)	(7)
	μ_{4f}	$\mu_{R\text{-cond}}$	μ_M	$\mu_{T\text{-cond}}$	$\mu_{R\,5d}$	$\mu_{M\,3d}$	$\mu_{diffuse}$
$GdFe_2$	7	0.91	−4.06	−3.15	0.65	−4.23	0.42
$TbFe_2$	9	0.81	−3.92	−3.11	0.58	−4.09	0.39
$DyFe_2$	10	0.75	−3.83	−3.08	0.53	−3.98	0.37
$HoFe_2$	10	0.68	−3.70	−3.02	0.47	−3.84	0.35
$ErFe_2$	9	0.62	−3.60	−2.99	0.43	−3.75	0.33
$TmFe_2$	7	0.56	−3.48	−2.93	0.38	−3.62	0.31
$YbFe_2$	4	0.52	−3.45	−2.93	0.35	−3.59	0.31

Figure 4. Comparison between the measured (Clark 1980) and calculated total magnetic moments for the series.

of 2.0 μ_B was reported. Since we calculate in these two cases 1.92 μ_B and 1.88 μ_B (table 3—neutron diffraction measures the 3d contribution to the moment), respectively, we cannot claim that agreement with experiment is very good. However the consistency between the experiments is not satisfactory and the Fe moment seems unlikely to be larger in $ErFe_2$ than in $HoFe_2$.

Finally we summarize the calculated total moments in figure 4 and compare them with the measured total moments (Clark 1980). The calculated total moments now include the small sp conduction band (or diffuse) contribution and the R 4f orbital contribution (table 1). Agreement with experiment is excellent, except for $YbFe_2$. In view of the excellent agreement for the rest of the series, $YbFe_2$ appears to be something of a puzzle. The data are not from single-crystal measurements as they are for $TmFe_2$–$TbFe_2$ (Clark 1980) but we calculate a smaller total moment than is measured and we suspect that this cannot be the explanation. However, the 4f spin moment is only 1 μ_B

in $YbFe_2$ and the corresponding exchange splitting of the 4f states is the smallest in the series. Crystal fields are therefore less likely to be a small perturbation to the exchange splitting and it may be that the 4f moment is quenched well below its free-ion (Russell–Saunders) value. If this were so the total calculated moment would be larger (see table 3), which would improve agreement with experiment.

4. Local exchange interactions

Exchange interactions appear in density functional theory via the spin potential, equation (2.2), but depending upon the kind of theory of interest the exchange inter-actions—or, more correctly, 'effective exchange interactions'—vary enormously. For example, experiments are often discussed in terms of molecular fields coupling the M 3d and R 4f moments (e.g. Beloritzky *et al* 1988), the corresponding effective exchange interactions being between M 3d and R 4f moments and probably quite different from the local exchange interactions in the LSDA. Similarly, Cyrot and Lavagna (1979) described finite-temperature magnetic properties of RM_2 compounds in terms of d–f and d–d interactions without distinguishing between R 5d and M 3d states. In this case also an effective exchange interaction between 3d and 4f states is important in the theory. Such effective—they actually arise from a combination of local exchange and 3d–5d hybridization—exchange interactions might be estimated from the change of splitting of the centres of the 3d bands with 4f moment in figure 2. Similarly figure 2 might be used to estimate the effective 4f–5d exchange interaction since the calculated splittings of the centres of the R 5d bands are also plotted as a function of 4f moment. If we take this as an example, then, since the exchange splitting of the centres of the 5d bands, δ_{5d}, is a linear function of the 4f and 5d spin contributions to the moment

$$\delta_{5d} = C_{5d}^+ - C_{5d}^- = J_{5d5d}\mu_{5d}^s + J_{4f5d}\mu_{4f}^s. \tag{4.1}$$

J_{4f5d} for $GdFe_2$ may be obtained directly from figures 2 and 3 where the exchange splittings and 5d moments are plotted for $GdFe_2$. We obtain

$$GdFe_2\ J_{4f5d} = 5.5\ mRyd \qquad J_{5d5d} = 49\ mRyd.$$

Furthermore, since μ_{5d}^s is itself a linear function of the μ_{4f}^s which from figure 3 we may write as

$$\mu_{5d}^s = 0.39 + 0.0383\mu_{4f}^s \tag{4.2}$$

we may rewrite (4.1) for $GdFe_2$ as

$$\delta_{5d} = 0.39 J_{5d5d} + (J_{4f5d} + 0.0383 J_{5d5d})\mu_{4f}^s. \tag{4.3a}$$

Therefore the 4f–5d exchange interaction is effectively enhanced by 5d–5d exchange, and so the 5d exchange splitting, regarded as a function of μ_{4f}^s, is given by

$$\delta_{5d} = 0.39 J_{5d5d} + J_{4f5d}'\mu_{4f}^s \tag{4.3b}$$

with

$$J_{4f5d}' = 7.38\ mRyd.$$

This enhancement of the bare 4f–5d exchange interactions is likely to enter most sys-tematic studies of exchange interactions across the series as, although (4.1) is the correct

expression, μ^S_{5d} is unlikely to be known and the dependence of δ_{5d} upon μ^S_{4f} alone is more likely to enter such theories.

Similarly, the moment decomposition in figure 3 may be used to evaluate the susceptibilities of the 3d and 5d moments to the 4f moments. If we write, for $GdFe_2$,

$$\mu_{5d} = \mu^{(0)}_{5d} + \chi_{5d4f}\mu_{4f} \qquad \mu_{3d} = \mu^{(0)}_{3d} + \chi_{3d4f}\mu_{4f}$$

we obtain

$$\chi_{5d4f} = 0.038/\text{FU} \qquad \chi_{3d4f} = 0.058/\text{FU}.$$

It is, however, possible to calculate the bare exchange integrals directly as in the LSDA version of Stoner–Wohlfarth theory. LSDA has long been used to provide a formal basis for the Stoner–Wohlfarth theory (Stoner 1938, Wohlfarth 1953) of itinerant magnetism (Gunnarsson 1976, 1977, 1978, Janak 1977, Vosko *et al* 1975, Vosko and Perdew 1975). The local exchange interactions between partial spin densities resolved according to angular momentum character are an intrinsic part of the theory. Here we are not so much interested in the enhanced paramagnetic susceptibility, which involves not only exchange integrals but also the partial state densities at the Fermi level (see e.g. Janak 1977, Vosko *et al* 1975, Vosko and Perdew 1975, Christensen *et al* 1988), but in the exchange interactions themselves (see also, e.g., Watson 1990, Gunnarsson 1976, 1977, Brooks and Johansson 1983). These are obtained approximately by first expanding the exchange-split potential, equation (2.2), to first order in the magnetic moment density which is resolved into its partial angular momentum components, assuming that spin-up and spin-down densities do not differ, that only states close to the Fermi level contribute to the magnetic moment, and applying first-order perturbation theory by averaging Δv_{xc} with the wave function at the energy for which the splitting is required. The energy splitting for the partial wave $\varphi_l(r, E)$ is then

$$\Delta\varepsilon_l(E) = \sum_{l'} J_{ll'}(E)\mu_l\mu_{l'} \tag{4.4}$$

in terms of the local exchange integral matrices given by

$$J_{ll'}(E) = \frac{2}{3}\int dr\, r^2\varphi_l^2(r, E_F)\varphi_{l'}^2(r, E)A(r)/n(r) \tag{4.5}$$

which are energy dependent. Usually the exchange integrals are evaluated at the Fermi energy since it is there that the splitting is required in a description of the magnetic instability. Then one obtains essentially the average splitting of the partial *l*-bands per unit of spin moment, $\mu_{l'}$, obtained from the potential difference (2.2) at the Fermi level. We have evaluated the integrals, $J_{ll'}(E_F)$, for the compounds $GdFe_2$–$YbFe_2$, using the self-consistently calculated densities and find that most of the exchange integrals are approximately constant across the series:

(a) at the M site: $J_{dd} = 61\,\text{mRyd}$ $J_{dp} = 20\,\text{mRyd}$ $J_{ds} = 23\,\text{mRyd}$

(b) at the R site: $J_{dd} = 43\,\text{mRyd}$ $J_{dp} = 44\,\text{mRyd}$ $J_{ds} = 46\,\text{mRyd}$

and J_{fd} varies smoothly from 6.8 mRyd for $GdFe_2$ to 5.7 mRyd for $YbFe_2$.

We have also calculated the splitting between the spin-up and spin-down states for each partial wave by taking the expectation value of (2.2) with the appropriate wave function, $\varphi(l, E_F)$, and found that the expansion leading to (4.4)—with the exchange integrals listed above—is accurate to a few per cent. For example, in $GdFe_2$, the

calculated magnitudes of the splittings of the R 5d and M 3d states at the Fermi level are 76 mRyd and 125 mRyd, respectively. Equation (4.4) yields 83 mRyd and 113 mRyd when all of the partial moments and exchange splittings are inserted. The importance of (4.4) and (4.5) is that they comprise the origin of the molecular fields that pervade model theories of magnetism in R–M intermetallics (see, e.g., Beloritzky *et al* 1988).

5. A sum rule for the conduction electron moment

A simplified model of the 3d and 5d partial state densities has been discussed in I. Here we start with the unhybridized 3d bands spin polarized and an exchange splitting δ_{5d} applied to the 5d states. It is a good approximation to assume that, before 3d–5d hybridization is introduced, the 5d bands are empty, and the 3d bands have occupation numbers n_{3d}^+, n_{3d}^- and fractional occupation numbers $f_{3d}^\pm = n_{3d}^\pm/N_{3d}$ where $N_{3d} = 20$ is the number of 3d spin states per primitive cell (containing two formula units).

When 3d–5d hybridization is introduced, the spin transfer to the 5d states is given, in the notation used in I, by

$$n_{5d}^\pm = f_{3d}^\pm M_{3d5d}^2 \Delta_{3d} \Delta_{5d}/(C_{3d}^\pm - C_{5d}^\pm)^2 \tag{5.1}$$

where the second moment of the hybridization structure constants, M_{3d5d}, and the bandwidth parameters, Δ_l, are defined in I and in papers by Andersen and his collaborators (Andersen *et al* 1978, 1979). These parameters are also listed, for the compounds under discussion, in table 2. Now the number of electrons of a given spin and total number of electrons transferred to the 5d states by hybridization with the 3d states is equal to the number of electrons lost by the 3d states, if redistribution at the Fermi level is small. We therefore have, using primed and unprimed quantities to denote before and after hybridization, respectively, the sum rule

$$n_{3d'}^\pm + n_{5d'}^\pm = n_{3d}^\pm + n_{5d}^\pm. \tag{5.2}$$

Since the 5d states are empty before hybridization, $n_{5d'} = 0$, and

$$n_{3d'}^\pm = n_{3d}^\pm + n_{5d}^\pm \tag{5.3}$$

Hence the moments obey the sum rule

$$\mu_{3d'} = \mu_{3d} + \mu_{5d}. \tag{5.4}$$

Therefore the total moment remains constant.

In I we have argued that the 3d and 5d moments must be anti-parallel (see also Yamada 1988, Szpunar 1985). This is easily seen to be so from (5.1). If δ_{5d} is zero the gap between the 3d and 5d spin-up bands is greater than the gap between the 3d and 5d spin-down bands. Therefore, by (5.1), the spin-up transfer to 5d bands is less than the spin-down transfer provided that f_{3d}^+, f_{3d}^- are not very different. The 3d and 5d moments are then anti-parallel. For RFe$_2$ systems there are about 13.5 3d electrons/FU (figure 1) with a moment/FU of about 4 μ_B, hence $f_{3d}^+ \simeq 0.9$ and $f_{3d}^- \simeq 0.5$. However, if a compound with a lighter transition metal with $\leqslant 10$ 3d electrons/FU were polarized completely, only f_{3d}^+ would be non-zero and the resulting 5d moment would be parallel to the 3d moment.

Since the 3d and 5d moments are antiparallel and the spin component of the 4f moment is parallel to the 5d moment (J_{4f5d} is always positive as are all local exchange interactions) the exchange splitting of the 5d states, given by (4.1), increases the spin-down transfer to 5d states and decreases the spin-up transfer. Hence an increasing 4f

moment increases *both the anti-parallel 3d and 5d moments.* However due to (5.4) *the total moment remains constant—independent of the 4f moment.* This explains the results shown in figure 3 for Gd-4f-red. It is also possible to see how the anti-parallel 3d–5d alignment leads to effective 4f–3d interaction. Since the 4f moment increases both 5d and 3d moments it increases the exchange (or spin-polarization) energy, which is proportional to the square of each moment. Since $\mu^s_{3d} \gg \mu^s_{5d}$, the dominant energy gain is from the increase in 3d moment. Therefore the effective interaction between 4f and 3d moments involves 4f–5d exchange, J_{4f5d}, the 3d exchange energy proportional to J_{3d3d}, and hybridization between 3d and 5d states. In addition there is the non-trivial kinetic energy contribution. We shall consider the effective 4f–3d interaction in more detail in another paper.

Finally in this section, we consider the effect of a uniform field applied to RFe_2 or a similar compound, starting with $LuFe_2$ where there is no 4f moment. Since in this case we are dealing with a spin-only system, 3d and 5d spin up levels are shifted equally down, and the spin-down levels are shifted equally up. Again from (5.1), there is no change in 3d–5d hybridization and no change in the fraction of spin transferred from 3d to 5d states. Thus the nature of the 5d moment, transferred from the 3d band by hybridization, prevents the 5d spin from being flipped in an applied field—a notion that arises from a localized model of the magnetism where the magnitude of the moments is fixed. What does happen is that the 3d moment increases in an applied field by an amount that depends upon the 3d high-field susceptibility. Then f^+_{3d} is increased and f^-_{3d} decreased and, from (5.1), the magnitude of the 5d moment decreases. The total increase in moment remains equal to the increase in μ^s_{3d} in (5.4). There will always be finite 5d$^-$ character as long as there is 3d$^-$ character, and total moment saturates when μ^s_{3d} saturates.

For the situation when there is a 4f moment at the R site that produces a splitting of the 5d states larger than the 3d splitting, the R moment may be flipped to parallel alignment with the 3d states. In this case, with the 5d splitting of opposite sign but greater in magnitude than the 3d splitting, the 5d$^+$, 3d$^+$ gap is reduced to be less than the 5d$^-$, 3d$^-$ gap. The 5d moment is then self-consistently parallel to the 3d moment as the spin-up transfer to 5d bands is, by (5.1), greater than the spin-down transfer and a metastable—completely ferromagnetic—state exists.

6. Conclusions

Two mechanisms through which localized R 4f moments may interact indirectly with M 3d moments in RM intermetallics have been proposed in the past on heuristic grounds. The RKKY (Ruderman and Kittel 1954, de Gennes 1962) interaction is naturally always a possibility when indirect exchange interactions are required. In fact a generic form of RKKY theory embraces the kind of indirect exchange interactions discussed in this paper—the polarization of conduction electron (of whatever partial angular momentum character) states at the Fermi level by local 4f–conduction electron exchange interactions and the propagation of the interaction by conduction electrons. However, RKKY theory was proposed for simple metals and does not lend itself well to the treatment of indirect exchange in compounds where it obscures the nature of the conduction electron bands. The proposal made by Campbell (1972), which distinguishes the local 5d character of the conduction electron moment at the R site and postulates that intersite interactions are 5d–3d interactions—of whatever nature—is a more useful way to characterize the

interactions between R 4f and M 3d states in compounds, as it recognizes the origin of the conduction band states. The energies of the pure M 3d scattering states span a range that is not degenerate with the energy range of the pure R 5d states and in this sense the R 5d states only become occupied by hybridization. Under these circumstances more physical insight is gained by analysing the conduction band structure in terms of 3d–5d hybridization than by using the complete energy band calculations to observe that there are conduction bands at the Fermi level through which the effect of local polarization by the 4f states must propagate. Fortunately LMTO theory provides an excellent basis set for the kind of analysis used in the simplified model of weak hybridization discussed in I and section 5.

One conclusion of this paper is that, although the total conduction electron moment in RFe$_2$ compounds is largely independent of the R 4f spin, the ferromagnetic site-resolved moments change significantly. We are at present analysing the change in energy with 4f moment and its interpretation in terms of 4f–3d interaction, the accuracy of the exchange integrals, $J_{ll'}$, and the contribution to molecular field theory. This work will be reported in a following paper.

Another conclusion at which we have arrived is that the 4f spin density may be successfully treated as part of a self-consistent outer core. The emphasis here is upon calculating the spin density correctly since that is all that enters LSDA. Since the 4f density is practically zero at the R Wigner–Seitz sphere there cannot be any appreciable change in 4f density between the top and bottom of any 4f bands, quite independently of whether electron correlation prevents such band formation or not. Secondly, the application of LSDA in calculating the spin-polarization energy of atoms (Gunnarsson *et al* 1974, Johansson *et al* 1980, Moruzzi *et al* 1978, Brooks 1983, Brooks and Johansson 1983, Brooks *et al* 1984) has been quite successful. Hence the exchange–correlation functionals used in LSDA should describe the spin-polarization energy quite well—even for localized states—and the splitting of the conduction electron states by the 4f spin density should be accurate. Nevertheless the comparison of the results obtained from calculations such as these with experiment is essentially a test of the LSDA. The rare earth–transition metal intermetallics provide a broad class of technologically important materials and magnetic data where LSDA may be tested when the 4f spin density is calculated. The results of the present calculations (and of those for the corresponding RCo$_2$ compounds which will be reported in the next paper of this series) provide grounds for optimism. Spin-polarized core calculations for solids have been rare. An early calculation by Malik *et al* (1977) for SmCo$_5$ seems to have suffered from convergence problems and the choice of spin contribution to the 4f moment. More recently Norman and Koelling (1986) successfully applied the method to CeSb although, in this case with one 4f electron, the problem of Russell–Saunders coupling was absent. We have also included the 4f states in the energy bands in several of the RFe$_2$ compounds. We do not report the results because, where they are different from those reported here, they are incorrect. Not only are the state densities close to the Fermi level far too high (other than for GdFe$_2$) but, more seriously, the Russell–Saunders coupling scheme is lost. This scheme, which reflects the correlated many-electron ground state of localized 4f states by imposing the correct rotational invariance under simultaneous rotations of all the 4f electrons, is an essential characteristic of the theory used here. The large orbital moment densities that may arise in the *narrow bands* of heavy elements (Brooks and Kelly 1983, Brooks 1985, Brooks *et al* 1988, Eriksson *et al* 1990) are obtained from a quite different coupling scheme and yield quite different magnetic moments.

Finally, it is worth mentioning that a combination of the methods used in this paper for the 4f spin density and the use of the non-spherical parts of the charge density at the

R site as implemented by Coehoorn (1990) provide a promising way of calculating the crystal-field effects upon the 4f states and, with them, the magnetic anisotropy of the compounds from first principles.

Acknowledgments

References

Andersen O K 1975 *Phys. Rev.* B **12** 3060
Andersen O K, Jepsen O and Glötzel D 1985 *Highlights of Condensed Matter Theory* ed F Bassani, F Fumi
      and M Tosi (Amsterdam: North-Holland)
Andersen O K, Klose W and Nohl H 1978 *Phys. Rev.* **17** 1209
Andersen O K, Skriver H L, Nohl H and Johansson B 1979 *Pure Appl. Chem.* **52** 93
Bargouth M O and Will G 1971 *J. Physique Coll.* **31** C1 675
Beloritzky E, Grigan J P, Grivord D and Li H S 1988 *Europhys. Lett.* **5** 349
Brooks M S S 1983 *J. Phys. F: Met. Phys.* **14** 1157
——— 1985 *Physica* **130** B 6
Brooks M S S, Eriksson O and Johansson B 1989 *J. Phys.: Condens. Matter* **1** 5861
Brooks M S S, Eriksson O, Johansson B, Franse J J M and Frings P H 1988 *J. Phys. F: Met. Phys.* **18** L33
Brooks M S S and Johansson B 1983 *J. Phys. F: Met. Phys.* **13** L197
Brooks M S S, Johansson B and Skriver H L 1984 *Handbook of Chemistry and Physics of the Actinides* ed A
      J Freeman and G H Lander (Amsterdam: North Holland)
Brooks M S S and Kelly M 1983 *Phys. Rev. Lett.* **51** 1708
Buschow K H J 1977 *Rep. Prog. Phys.* **40** 1179
Buschow K H J, Van Diepen A M and de Wijn H W 1973 *Phys. Rev.* B **8** 5134
Campbell I A 1972 *J. Phys. F: Met. Phys.* **2** L47
Christensen N E, Gunnarsson O, Jepsen O and Andersen O K 1988 *J. Physique Coll.* **49** C8 17
Clark A E 1980 *Ferromagnetic Materials* ed E P Wohlfarth (Amsterdam: North-Holland) p 297
Coehoorn R 1990 *Supermagnets, Hard Magnetic Materials (Lecture Notes Nato-ASI)* ed G J Long and F
      Grandjean (Dordrecht: Kluwer)
Cyrot M and Lavagna M 1979 *J. Physique* **40** 763
de Gennes P G 1962 *J. Physique Radium* **23** 510
de Wijn H W, Van Diepen A M and Buschow K J H 1976 *Phys. Status Solidi* **76** 13
Dimmock J O and Freeman A J 1964 *Phys. Rev. Lett.* **13** 750
Duthie J C and Pettifor D G 1977 *Phys. Rev. Lett.* **38** 564
Eriksson O, Brook M S S and Johansson B 1990 *Phys. Rev.* B **41** 9087
Fuess H, Givord D, Gregory A R and Schweizer J 1979 *J. Appl. Phys.* **50** 2000
Gunnarsson O 1976 *J. Phys. F: Met. Phys.* **6** 587
——— 1977 *Physica* B **91** 329
——— 1978 *J. Appl. Phys.* **49** 1399
Gunnarsson O, Lundqvist R I and Wilkins J W 1974 *Phys. Rev.* B **10** 1319
Gunnarsson O and Schönhammer K 1983 *Phys. Rev.* B **28** 4315
——— 1985 *Phys. Rev.* B **31** 4815
Harmon B N 1979 *J. Physique Coll.* **40** C5 65
Herbst J F, Lowy D N and Watson R E 1972 *Phys. Rev.* B **6** 1913
Hohenberg P and Kohn W 1964 *Phys. Rev.* **136** 864
Hubbard J 1963 *Proc. R. Soc.* A **276** 238
Janak J F 1977 *Phys. Rev.* B **16** 255
Johansson B 1974 *J. Phys. F: Met. Phys.* **4** L169
——— 1979 *Phys. Rev.* B **20** 1315
Johansson B, Skriver H L, Mårtensson N, Andersen O K and Glötzel D 1980 *Physica* B **102** 12

Keaton S C and Loucks T L 1966 *Phys. Rev.* **146** 429
Kohn W and Sham L J 1965 *Phys. Rev.* A **140** 1133
Liu S H 1978 *Handbook on the Physics and Chemistry of Rare Earths* vol 1, ed K A Gschneidner Jr and L Eyring (Amsterdam: North-Holland) p 233
Malik S K, Arlinghaus F J and Wallace W E 1977 *Phys. Rev.* B **16** 1242
Moreau J M, Michel C, Simmons M, O'Keefe T J and James W J 1971 *J. Physique* **32** C1 670
Moruzzi V L, Janak J F and Williams A R 1978 *Calculated Electronic Properties and Metals* (New York: Pergamon)
Norman M R and Koelling D D 1986 *Phys. Rev.* B **33** 6730
Ruderman and Kittel C 1954 *Phys. Rev.* **96** 99
Skriver H L 1983 *Muffin Tin Orbitals and Electronic Structure* (Heidelberg: Springer)
Sticht and Kübler J 1985 *Solid State Commun.* **53** 529
Stoner E C 1938 *Proc. R. Soc.* **165** 372
Szpunar B 1985 *Physica* B **130** 29
Temmerman W M and Sterne P A 1990 *J. Phys: Condens. Matter* **2** 5529
von Barth U and Hedin L 1972 *J. Phys. C: Solid State Phys.* **5** 1629
Vosko S H and Perdew J P 1975 *Can. J. Phys.* **53** 1385
Vosko S H, Perdew J P and MacDonald A H 1975 *Phys. Rev. Lett.* **35** 1725
Watson R E 1990 *J. Appl. Phys.* **67** 5535
Wohlfarth E P 1953 *Rev. Mod. Phys.* **25** 211
Yamada H 1988 *Physica* B **144** 390